Tailoring Dynamic Hydrogels by Controlling Associative Exchange Rates

Vivian Zhang,[1] Joseph V. Accardo,[1] Ilia Kevlishvili,[2] Eliot F. Woods,[1] Steven J. Chapman,[1] Christopher T. Eckdahl,[1] Heather J. Kulik,[2] Julia A. Kalow[1]

[1]Department of Chemistry, Northwestern University, 2145 Sheridan Road, Evanston, IL 60208, United States of America

[2]Department of Chemical Engineering, Massachusetts Institute of Technology, 25 Ames Street, Cambridge, MA 02142, United States of America

ABSTRACT: Dithioalkylidenes are a recently-developed class of conjugate acceptors that undergo thiol exchange via an associative mechanism and have been used for reprocessable vitrimers, amine sensors, and degradable networks. Here, we show that the exchange rate of the reaction in aqueous environments is highly sensitive to the structure of the acceptor and may be varied over four orders of magnitude. Cyclic acceptors exchange rapidly, from 0.95 to 15.6 $M^{-1}s^{-1}$, while acyclic acceptors exchange between $3.77x10^{-3}$ and $2.17x10^{-2}$ $M^{-1}s^{-1}$. Computational, spectroscopic, and structural data suggest that the cyclic acceptors are more reactive than their linear counterparts because of resonance stabilization of the tetrahedral intermediate. We leverage this insight to design a compound with reactivity intermediate to that of the cyclic and linear analogs. Lastly, we incorporate this dynamic bond into hydrogels and demonstrate that molecular k_{ex} correlates with the hydrogel's characteristic stress relaxation time (τ); furthermore, these values may be parametrized with respect to computed descriptors of the electrophilic site. This work opens new avenues to design and control hydrogel viscoelasticity with an associative exchange mechanism.

INTRODUCTION

The physical properties of polymer networks may be varied over a vast range simply by changing the identity of their cross-links. Insight into the relationship between cross-link structure and bulk properties empowers chemists to precisely design materials suitable for a myriad of applications.[1,2] Hydrogels, three-dimensional (3D) hydrophilic networks swelled with water, are a ubiquitous class of soft materials used across agriculture, personal care products, and biomedicine.[3] Imparting viscoelasticity (both solid- and liquid-like behaviors) into hydrogels enables desirable features such as stress relaxation (adaptation to applied strains) and stimuli responsiveness.[4,5] In biomedical fields, engineered cell culture scaffolds with biomimetic mechanical properties have transformed how cell-matrix interactions and downstream processes are studied, motivating the development of hydrogel systems where stress relaxation can be controlled independently from other network properties.[6–9] To predictively tailor hydrogel network properties through chemical design, we must first establish quantitative relationships between cross-link structure, molecular reactivity, and macromolecular stress relaxation.

Viscoelasticity arises in part from cross-link rearrangement, which can occur through dissociative or associative mechanisms. The mechanism has implications on how network stiffness and stress relaxation are coupled (**Figure 1a**). The majority of viscoelastic hydrogels are based on dissociative dynamic interactions, such as hydrophobic association,[10,11] host-guest complexation,[12–14] hydrogen bonding,[15] or hydrolyzable dynamic covalent bonds like boronic esters and imines.[16–19] In dissociative networks, stiffness, a property determined by cross-link density, is related to K_{eq} (k_a/k_d) of the cross-link because it defines the proportion of bound to unbound cross-links at equilibrium. The self-healing rate depends on the rate of cross-link association (k_a), whereas stress relaxation is related to the rate of cross-link dissociation (k_d), the first step of network rearrangement.[20–22] Because K_{eq} is defined by k_a and k_d, it is challenging to design dissociative reactions for crosslinks in which rate and equilibrium constants, and therefore network stress relaxation and stiffness, can be independently manipulated.[16,23] The interdependence of these properties can be represented on a non-normalized stress relaxation plot, where a modification to k_d would typically result in changes to both the characteristic timescale of stress relaxation (τ), and the initial modulus (G_0), which describes stiffness.

To bypass the codependence of these properties in dissociatively-exchanging networks, we sought to develop hydrogels based instead on *associative* dynamic covalent exchange, following precedent from the field of reprocessable networks. Dry networks based on associative exchange mechanisms, or vitrimers, have gained attention due to their ability to undergo reprocessing while maintaining cross-link density.[24] Inspired by "declick" reactions developed by Anslyn and coworkers,[25] we previously developed PDMS vitrimers based on the conjugate addition–elimination of thiols to dithioalkylidene cross-links (**Figure 1b**).[26] We further demonstrated that the rate of vitrimer stress relaxation could be varied over four orders of magnitude without affecting stiffness by using different conjugate acceptor cross-linkers.[27]

These studies motivated us to develop hydrogels cross-linked with associatively-exchanging dithioalkylidenes. We envisioned tailoring the exchange rate k_{ex} to tune stress relaxation while the cross-link density that determines stiffness is unaffected. Meldrum's acid-derived dithioalkylidenes have been incorporated into chemically-responsive hydrogels, but stress relaxation (if present) was not characterized.[28–30] Thioesters, which exchange through an associative mechanism, have been used as dynamic cross-links in stress-relaxing hydrogels, but thioester exchange is extremely slow ($t_{1/2}$ > 30 h) at

physiological pH in the absence of a catalyst, leading to slow stress relaxation.[31–34]

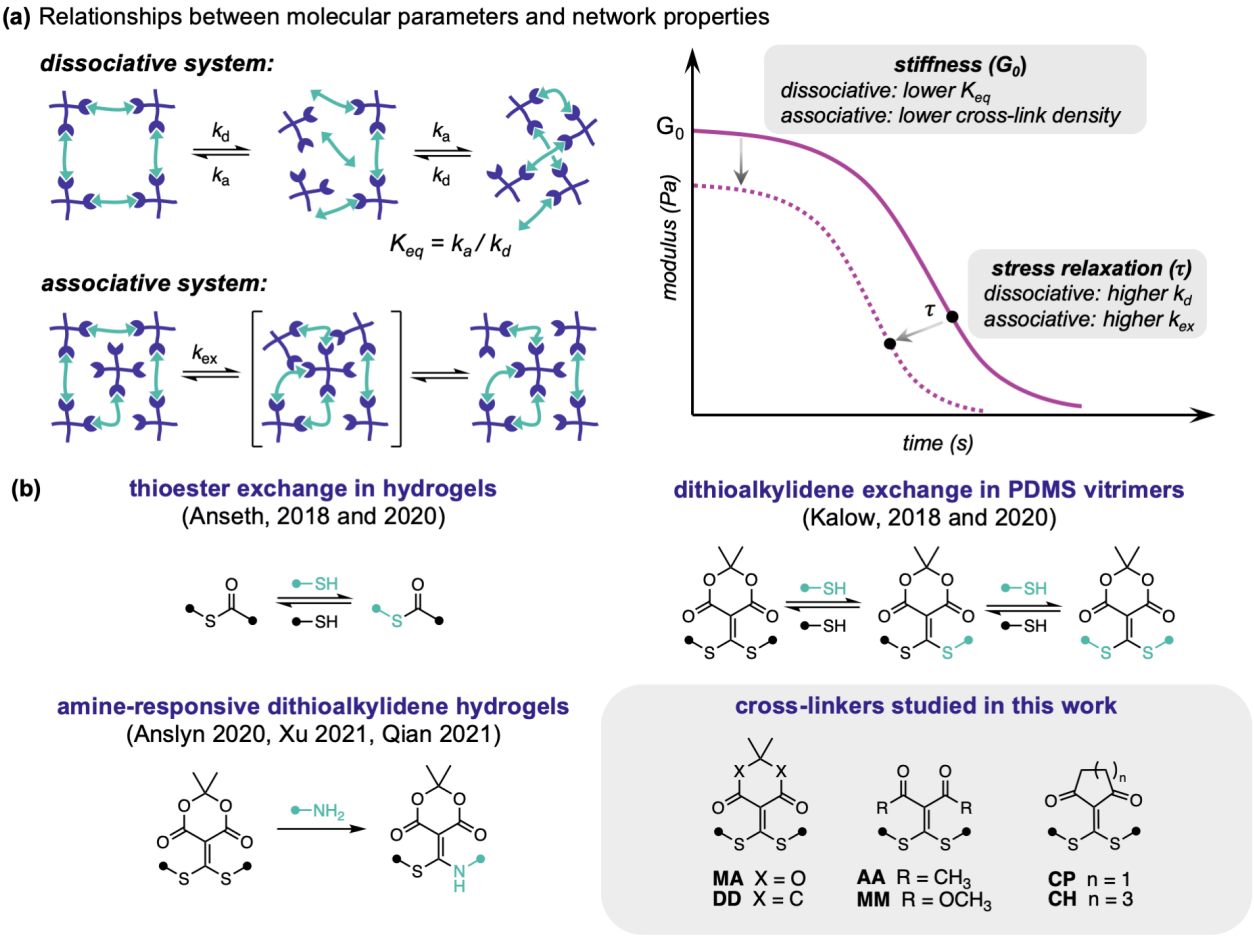

	this work	Kalow, 2018 and 2020	Anseth, 2018 and 2020	Anslyn 2020 Xu 2021[a] Qian 2021
aqueous conditions	✓		✓	✓
stress-relaxing materials	✓	✓	✓	
range of timescales achieved (τ)	10^{-1} – 10^{3} s (23 °C)	10^{1} – 10^{4} s (100–150 °C)	10^{4} – 10^{6} s (23 °C)	N/A

Figure 1. (a) Comparison between dissociative and associative exchange mechanisms and their effects on macroscopic network properties. In dissociative systems, the binding constant (K_{eq}) determines stiffness (G_0) while the rate of dissociation (k_d) determines viscoelasticity. In associative systems, the cross-link density, determined by synthesis conditions, dictates stiffness, while exchange rate (k_{ex}) determines viscoelasticity. (b) Examples of associative thiol exchange reactions applied to hydrogels and vitrimers. In this work, a range of conjugate acceptors are synthesized from organic diacids to study the aqueous exchange mechanism of dithioalkylidenes and translate these effects to hydrogel viscoelasticity. [a]In ref. [30], hydrogels with excess thiol are qualitatively self-healing, but stress relaxation is not characterized.

Here, we investigate the relationship between conjugate acceptor structure, k_{ex}, and viscoelasticity for conjugate addition–elimination using a series of dithioalkylidenes and their corresponding hydrogels (**Figure 1b**). Though we previously observed cross-link-dependent effects on stress relaxation for vitrimers, we did not measure the small-molecule exchange rates for the cross-links employed. In order to quantitatively evaluate the relationship between molecular reactivity and network properties, these kinetic data are required. We therefore measured the molecular exchange rates under aqueous conditions and used computational and experimental data to rationalize structure-dependent changes in reactivity. The exchange rates may be quantitatively correlated to computed molecular parameters. By incorporating the corresponding cross-links into photopolymerized hydrogels, we further demonstrated that the hydrogel's stress relaxation time (τ) is directly proportional to molecular k_{ex}. We leveraged this insight to design a compound and computationally

appraise its reactivity and relaxation timescale. Overall, we demonstrate that mechanistic insight into cross-link exchange and parametrization of cross-link reactivity enables the design of materials with targeted viscoelasticity.

RESULTS AND DISCUSSION

Kinetic measurements of dithioalkylidene exchange in aqueous media. We sought to synthesize and measure exchange rates for a library of dithioalkylidene structures (generically abbreviated **XL**) to evaluate the compatibility of this exchange reaction with associatively-exchanging, stress-relaxing hydrogels. We therefore designed the non-degenerate small molecule model system shown in **Figure 2a** to mimic cross-link conjugate exchange. Water-soluble **XL-1** was dissolved in an 8:2 mixture of aqueous HEPES buffer (0.1 M, pH 7.44) and acetonitrile and subjected to 2 equiv of a chemically distinct thiol **BT** to generate singly- and then doubly-exchanged products **XL-2** and **XL-3**. The concentrations of each species were monitored over time using reverse-phase high-performance liquid chromatography (RP-HPLC) until equilibrium was reached.

We first began our investigation with compound **MA-1** and observed that the concentrations of **MA-1**, **-2**, and **-3** approached a 1:2:1 ratio as the reaction approached equilibrium over ca. 30 minutes, indicating that **BT** and **ET** have comparable reactivity. The second-order rate constant (k_{ex}) for associative exchange of **MA-1** with **BT** was determined to be 6.65 ± 0.85 $M^{-1}s^{-1}$ (see SI for details of derivation and fit). We independently synthesized **MA-3** and performed the reverse reaction to confirm that **BT** and **ET** exhibit comparable exchange rates (SI, **Figure S1**).

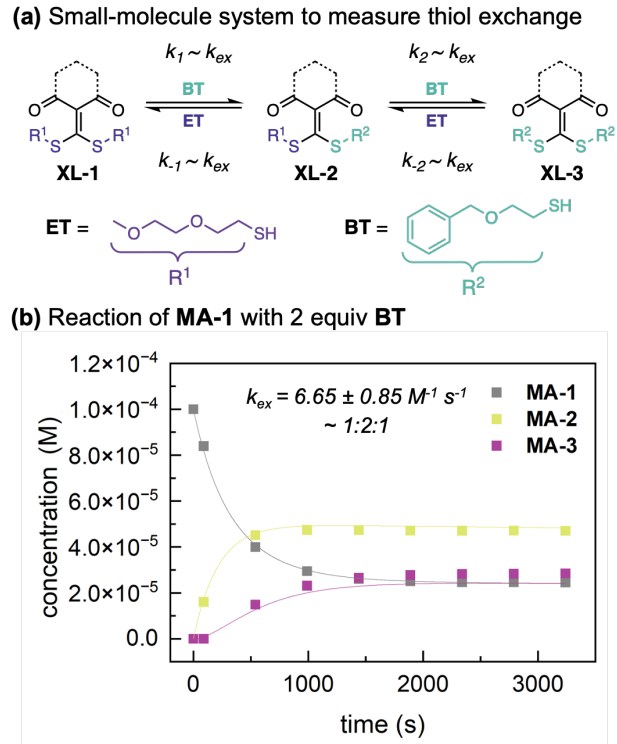

Figure 2. (a) The non-degenerate reaction used to monitor the exchange process with various cross-linkers (**XL**). (b) Representative kinetic profile for the equilibration of 100 μM of **MA-1** with 200 μM **BT** to generate a 1:2:1 mixture of **MA-1–3**. Curves show fit to the second-order kinetic model.

We next synthesized diketones **DD-1** and **CP-1** from dimedone and 1,3-cyclopentanedione, respectively, to determine how ring size and carbonyl class influence the rate of exchange. Equilibration of these compounds with 2 equiv **BT** occurred within an hour, with the disappearance of starting material following the trend **CP** > **MA** > **DD**. Inspection of the concentration versus time data, however, revealed a gradual decrease in the total concentration of dithioalkylidene species for **CP-1** and **DD-1**, which was not observed for **MA-1** on the same timescale. Jewett and coworkers previously used related diaminoalkylidenes derived from Meldrum's acid as tools for the irreversible modification of amines in basic solution. They discovered that these compounds react reversibly with hydroxide anions to form a stable adduct at high pH (**Figure 3a**).[35] We therefore hypothesized that **DD-1** and **CP-1** react analogously with hydroxide but undergo irreversible loss of thiol (**Figure 3b**). Control experiments with **DD-1** or **CP-1** in the absence of **BT** confirm a slow, linear decrease in concentration as a function of time (SI, **Figure S9**), and the hydrolysis products were confirmed by mass spectrometry. The kinetic model was modified to include the hydrolysis pathway for **DD** and **CP** (details in SI), and k_{ex} values were thus determined to be 0.95 ± 0.0046 and 15.6 ± 0.45 $M^{-1}s^{-1}$, respectively (**Figure 4a**). The non-negligible hydrolysis of **DD** and **CP** within the time frame of the kinetic experiments limit their use as cross-links in hydrogels.

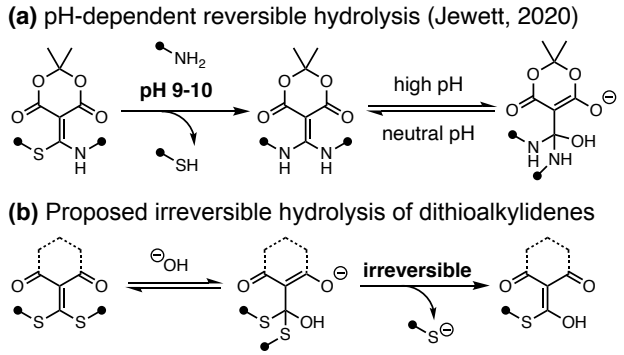

Figure 3. (a) pH-dependent amine addition to Meldrum's acid-derived diaminoalkylidenes and reversible hydrolysis in aqueous solution. (b) Proposed hydrolysis of dithioalkylidenes in water.

Based on our previous studies of stress relaxation in PDMS vitrimers,[27] we hypothesized that dithioalkylidenes derived from linear 1,3-diketones and diesters would undergo exchange more slowly than their cyclic analogs. However, we anticipated that the calculated gas-phase exchange mechanism may not apply to the aqueous environments of interest here. Compounds **MM** and **AA** were synthesized from dimethyl malonate and acetoacetone as linear analogs of **MA** and **DD**/**CP.** Under the standard second-order reaction conditions with 2 equiv of **BT**, **MM-1** and **AA-1** failed to show measurable conversion over multiple days. Therefore, we instead employed pseudo-first-order conditions with 20–100 equiv **BT** to measure k_{ex} for these linear dithioalkylidens (**Figure 4b**). Second-order rate constants for k_{ex} of **MM-1** and **AA-1** were determined to be 3.77 x 10^{-3} and 2.17 x 10^{-2} $M^{-1}s^{-1}$, respectively, which are 2–4 orders of magnitude slower than those of the cyclic acceptors (**Figure 4c**). These data demonstrate the highly sensitive relationship between cross-link structure and k_{ex}.

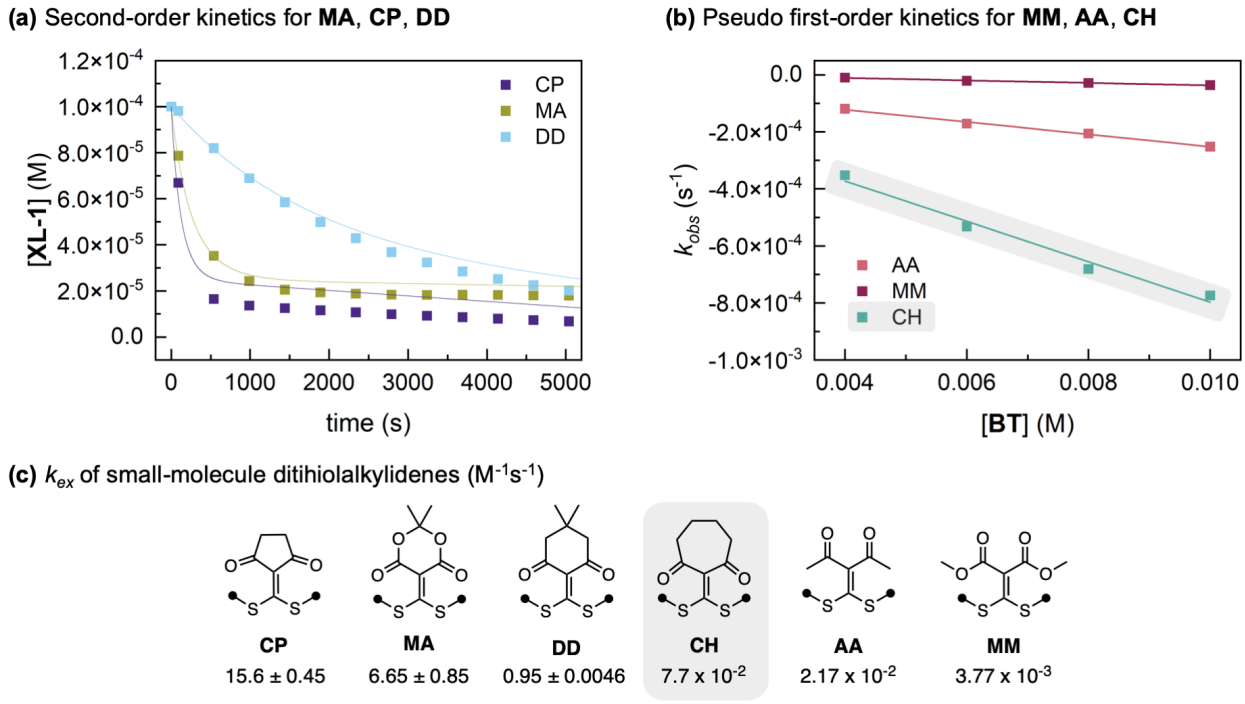

Figure 4. Structure-reactivity trend for a library of dithioakylidenes determined using a quasi-degenerate thiol exchange reaction. (a) Concentration versus time traces for the disappearance of 100 μM **MA-1** (green), **DD-1** (blue), or **CP-1** (purple) with 200 μM **BT** in 8:2 aqueous HEPES (0.1 M, pH 7.44)–acetonitrile. Curves show fit to the second-order kinetic model incorporating hydrolysis. (b) k_{obs} versus [**BT**] to determine k_{ex} for **AA-1** (pink), **MM-1** (maroon), and **CH-1** (teal) (100 μM **XL-1** in 8:2 aqueous HEPES (0.1 M, pH 7.44)–acetonitrile) with 20–100 equiv **BT**. Lines show fit to a pseudo-first-order kinetic model. (c) Summary of k_{ex} values for cyclic and linear acceptors. Shaded boxes denote a structure and corresponding data for which the reactivity was first calculated *in silico* before experimental confirmation (*vide infra*).

Mechanistic rationale. In order to design cross-linkers with targeted exchange rates, we sought to understand the structure-dependent changes in k_{ex}. We envisioned that at pH 7.44, the reaction could occur through either a neutral or anionic pathway. Previously, we used gas-phase density functional theory (DFT) calculations to rationalize the difference in reactivity between cyclic and linear dithioalkylidenes in a nonpolar PDMS matrix.[27] Those studies implicated a neutral pathway, wherein cyclic acceptors experience lower activation energies for thiol addition due to the participation of the carbonyl as an internal base that activates the incoming thiol as it attacks in a closed transition state (**Figure 5a**). For linear acceptors, this closed transition state was unfavorable and thus internal catalysis could not occur.

However, our kinetic data suggest that the aqueous system may favor a different pathway. In the PDMS vitrimers, **DD** underwent stress relaxation ~70x faster than **MA**. In the aqueous experiments described here, **MA** exchanged ~7x faster than **DD**. To provide experimental evidence for reaction through an anionic pathway (**Figure 5b**), we measured exchange rates of **MA-1** with **BT** in aqueous HEPES buffer (0.1 M, pH 7.0–8.0). We observed a clear pH dependence, with k_{ex} increasing as a function of pH (**Figure 5c**). These results suggest that the anionic exchange pathway is favored under aqueous conditions; increasing pH increases the concentration of thiolate and thus accelerates the reaction. These results can be rationalized in analogy to the well-studied thiol-thioester exchange, which is known to proceed in part through a thiolate pathway in water.[33,34] DFT calculations for both **DD** and **AA** in water (conductor-like polarizable continuum model) further corroborated our experimental observations (see SI for details).

The proposed anionic mechanism for dithioalkylidene exchange under aqueous conditions is thus distinct from the neutral mechanism proposed for PDMS vitrimers. For an anionic mechanism, internal catalysis in a closed transition state cannot be implicated because the thiol proton is not present in the rate-limiting step. Therefore, we performed computational and spectroscopic studies to understand the origin of rate differences for this series of dithioalkylidenes.

We calculated energy-minimized structures for **MA**, **DD**, **CP**, **AA**, and **MM** and their anionic tetrahedral intermediates following addition of methanethiolate using DFT (see SI for details). Based on conformational analysis using the Conformer-Rotamer Ensemble Sampling Tool, the linear dithioalkylidenes had many more accessible conformers (19 to 29) compared to the cyclic acceptors (3 to 6), as expected based on the greater degrees of freedom for linear acceptors. While methanethiolate addition is endergonic for all dithioalkylidenes, it is less endergonic for the cyclic compounds. Indeed, there was a reasonable correlation between calculated ΔΔG for addition and the experimental $\Delta\Delta G^{\ddagger}$ determined from the measured exchange rates, consistent with the Bell–Evans–Polyani principle (**Figure 6a**; SI, **Table S9**). We next used the lowest-energy conformer of each tetrahedral intermediate to optimize transition state geometries for thiolate addition to each dithioalkylidene. The calculated $\Delta\Delta G^{\ddagger}$ values were also consistent with the experimental data (**Figure 6b**; SI, **Table S9**). Notably, for both calculated ΔΔG and $\Delta\Delta G^{\ddagger}$ values, **MA** was an outlier when compared to experimental trends. The anomalously low pKa of Meldrum's acid (7.3 in DMSO) has long been debated in computational studies and may point to

factors influencing the exchange rate that cannot be captured by the methods used here.[36–40]

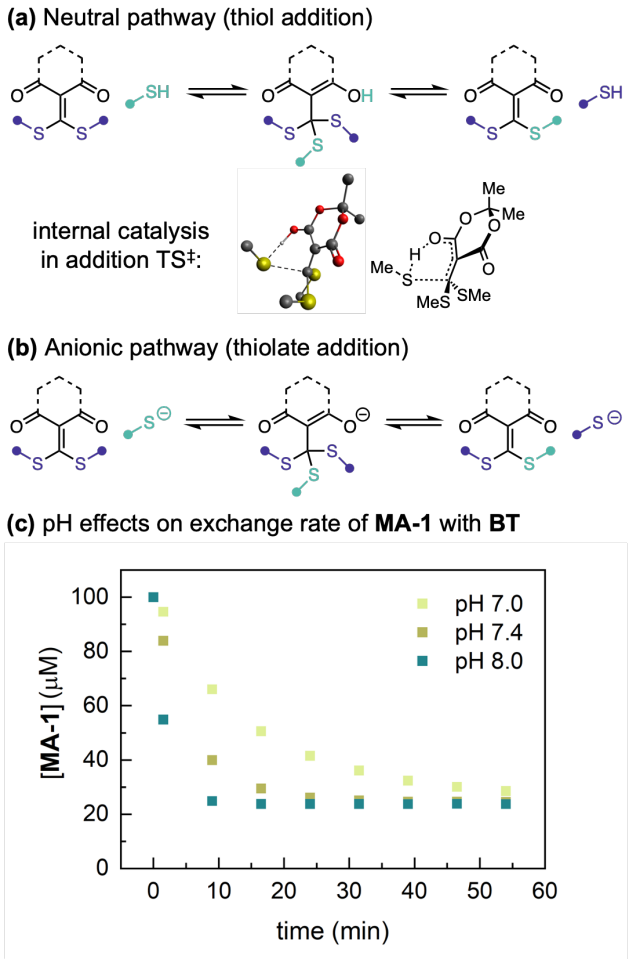

Figure 5. Proposed mechanisms for exchange through addition of (a) neutral thiol or (b) thiolate. (c) Increasing solution pH increases the exchange rate for **MA-1**.

Inspection of the transition states revealed that the cyclic dithioalkylidenes generally featured earlier transition states, with longer distances between the incoming nucleophile and the acceptor's β carbon, compared to their linear counterparts. For example, the C···S distance is 2.80 Å in the **DD** TS and 2.46 Å in the **AA** TS (**Figure 6c**). These differences suggest that the linear dithioalkylidenes react via more product-like transition states compared to more reactant-like transition states for the cyclic dithioalkylidenes (SI; **Table S8**). These trends are consistent with Hammond's postulate given the more endothermic addition to linear dithioalkylidenes. We thus conclude that the stabilization of the anionic tetrahedral intermediates governs the overall exchange rate. The conformationally restricted structure of the cyclic acceptors provides greater resonance stabilization of the anionic tetrahedral intermediate. In contrast, the linear dithioalkylidenes can adopt numerous ground-state conformations with respect to the carbonyls.

Increased polarization between the α and β carbons in cyclic dithioalkylidenes compared to linear ones were verified experimentally through ^{13}C NMR spectroscopy, crystallography, and UV-vis spectroscopy. For example, we observe similar ^{13}C NMR shifts for the α and β carbons of linear diketone **AA** (148 and 147 ppm, respectively), compared with significantly more shielded C_α and deshielded C_β signals for **CP** (122 and 194 ppm, respectively) (**Figure 7**). This trend is also observed when comparing **MM** and **MA** and suggests that the C=C π bonds are more polarized in the cyclic compounds. This conclusion is further supported by single-crystal X-ray structures of **CP**, **AA**, **MA**, and **MM**, which reveal longer C=C bonds and larger $SC_\alpha C_\beta C(O)$ dihedral angles for the cyclic compounds. Greater resonance stabilization for cyclic dithioalkylidenes is also reflected in red-shifted λ_{max} for the π–π^* transition in UV-vis absorption (SI, **Figure S15**). While we were unable to observe any tetrahedral intermediates spectroscopically, we can infer that the resonance stabilization in the dithioalkylidene reactant will be even more significant in the corresponding anionic intermediate. Therefore, we believe that these spectroscopic and structural descriptors of resonance stabilization trends are reasonable proxies for resonance stabilization of the intermediates, which dictates exchange rate.

Based on these trends, we sought a single, computationally derived descriptor of resonance stabilization that could be used to predict exchange rates. We first applied intrinsic atomic orbital (IAO) analysis,[41,42] which allows localized bonding orbitals to be assigned to a specific atom, to the lowest energy conformer of each dithioalkylidene. This analysis shows how the two electrons in the π bond are delocalized across the $C_\alpha C_\beta C(O)$ π system (SI, **Figure S11**). Compounds that exchange faster demonstrated decreased electron density at the β carbon, but the percent charge contributions did not correlate linearly with observed reaction rates. Therefore, we evaluated additional electronic descriptors and found that Hirshfeld charges of the dithioalkylidene β carbon (**Figure 8a**) and LUMO (**Figure 8b**) are well correlated to the experimental exchange rates. Other descriptors, such as HOMO value or condensed electrophilic Fukui function based on Hirshfeld charges, showed worse correlation (SI, **Figure S35**). The Hirshfeld charge intrinsically describes the difference between the molecular and charge density from the promolecule (i.e. the constituent atoms). Hirshfeld charges have been used to predict electrophilicity for electrophilic aromatic substitution and to generate a quantitative scale of electrophilicity and nucleophilicity.[43–45]

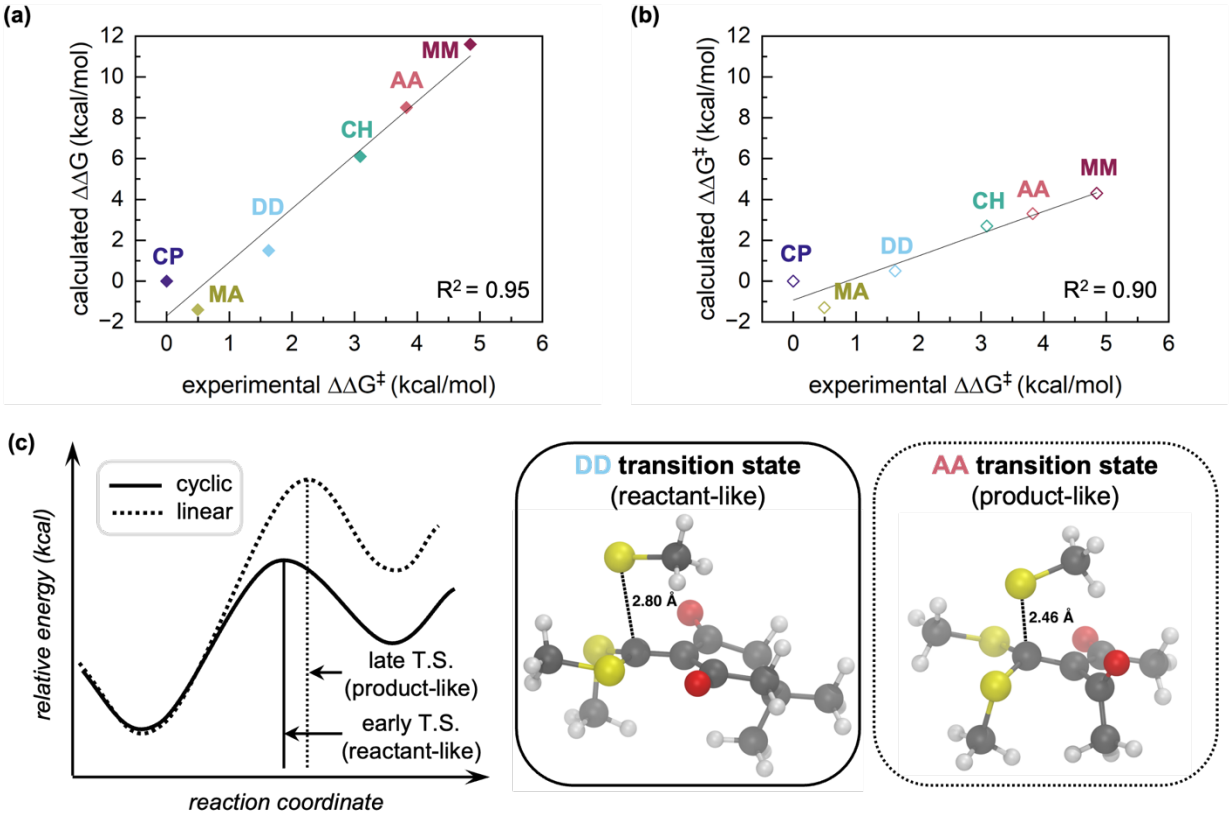

Figure 6. Computed thermodynamics and energies for methanethiolate addition to all **XL**s. (a) Correlation between calculated and experimental $\Delta G^{\ddagger}$ normalized to **CP**. (b) Correlation between calculated ΔG for addition and experimental $\Delta G^{\ddagger}$ normalized to **CP**. (c) Qualitative reaction landscapes comparing thiolate addition to cyclic and linear dithioalkylidenes. Geometry optimizations of transition states performed at CAM-B3LYP/def2-SVPD-cpcm(water) level of theory demonstrate that the nascent bond is longer for cyclic **DD** (2.80 Å) than for linear **AA** (2.46 Å).

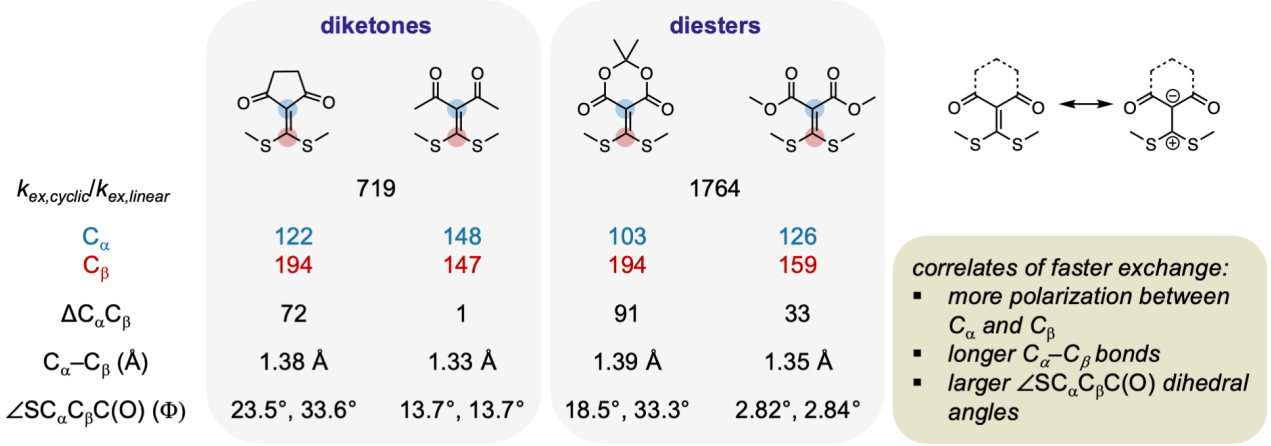

Figure 7. Structural comparisons of cyclic vs. linear diketone and diester C_α–C_β π bond obtained from ^{13}C NMR and single-crystal X-ray crystallography.

Predicting reactivity of a dithioalkylidene acceptor *in silico*. To demonstrate that these structure-reactivity relationships are indeed predictive, we designed an acceptor *in silico* that was predicted to provide reactivity intermediate to the cyclic and linear dithioalkylidenes. **CH** is a 7-membered cyclic diketone that is more flexible than **DD** and **CP**. Additionally, **CH** maintains the cyclic conformation that would enable internal catalysis and a closed transition state in the neutral pathway, and can provide additional support for or against the proposed anionic mechanism. Indeed, the calculated Hirshfeld charge for C_β in **CH** is 0.0161, which is greater than but more similar to the linear dithioalkylidenes (0.006–0.0102) compared to the cyclic ones (0.0344–0.0361) (**Figure 8a**; SI, **Table S10**). Similarly, the calculated LUMO value for **CH** is -0.0685, which also falls between that of the cyclic and linear values (SI, **Table S10**). The predicted reaction rates of **CH** based on the linear

trend of log(k_{ex}) against Hirshfeld charge and LUMO values (SI, **Figure S36**) are 5.6 x 10^{-2} $M^{-1}s^{-1}$ and 4.1 x 10^{-2} $M^{-1}s^{-1}$, respectively.

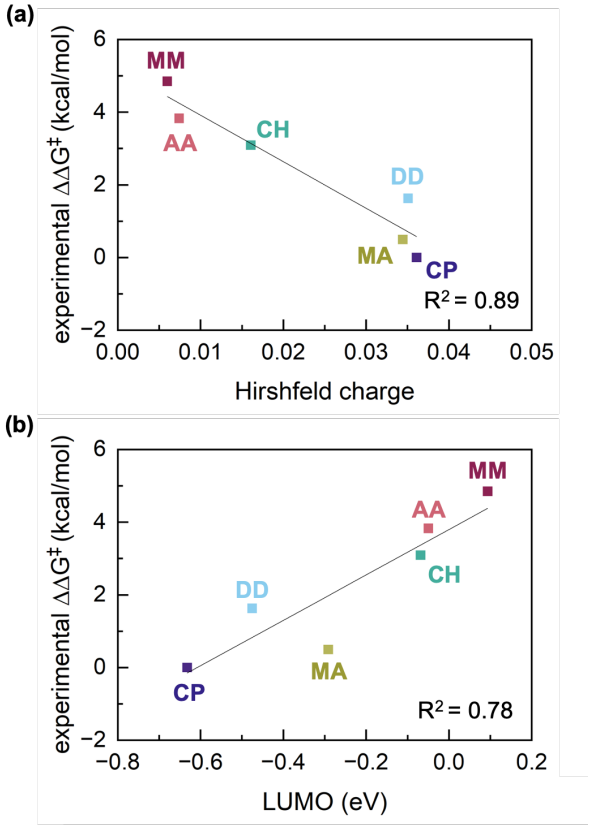

Figure 8. Correlating experimental $\Delta G^{\ddagger}$ normalized to CP with (a) Hirshfeld charge at C_β and (b) calculated LUMO (eV) of each dithioalkylidene.

Encouraged by this result, we synthesized **CH** from 1,3-cycloheptanedione (see SI for synthetic details) and noted that the C_α and C_β ^{13}C shifts appear at 140 and 160 ppm, consistent with π bond polarization intermediate to linear diketone **AA** and cyclic diketones **DD**/**CP**. Furthermore, UV-Vis absorption revealed λ_{max} intermediate to the linear and cyclic dithioalkylidenes (SI, **Figure S15**). Water-soluble derivative **CH-1** was then prepared and subject to the second-order kinetic assay with 2 equiv **BT**, which failed to show any appreciable conversion. Gratifyingly, the kinetic analysis with excess **BT** under pseudo first-order conditions revealed an exchange rate of 7.7 x 10^{-2} $M^{-1}s^{-1}$ (**Figure 4b**), comparable to the predicted k_{ex} values. Thus, the flexible cyclic acceptor **CH** undergoes exchange 12 times slower than **DD** and 3.5 times faster than **AA**.

Synthesis and characterization of stress-relaxing hydrogels. We next incorporated these dithioalkylidene derivatives as cross-linkers in stress-relaxing hydrogels to investigate the relationship between τ and k_{ex} in associative covalent adaptable networks. We first attempted to fabricate hydrogels by combining mercapto-terminated multi-arm poly(ethylene glycol) with dithioalkylidenes, wherein displacement and evolution of methanethiol would lead to gelation. This route was limited by the wide range of exchange rates: because gelation was contingent on thiol exchange, gelation with the linear cross-linkers was prohibitively slow. In order to form the network rapidly independent of the exchange chemistry, we designed cross-linkers **MA-4**, **AA-4**, **CH-4**, and **MM-4** with PEG-linked norbornene units, which can engage in rapid thiol-ene reactions (**Figure 9a**).[32] These dithioalkylidenes were selected based on the absence of competitive hydrolysis and the range of exchange rates they represent. **Ctrl** was synthesized as a control cross-link that cannot undergo associative exchange after cross-linking.

To form hydrogels, either **MA-4**, **MM-4**, **AA-4**, **CH04**, or **ctrl** was added to a solution of 4-arm PEG-SH (M_w 5 kDa) with a norbornene:thiol ratio of 1:2 to achieve a final polymer concentration of 10 w/v% in methylene chloride. When the ratio of norbornene to thiol is less than 1, free thiols are available to participate in the exchange reaction. Eosin Y was added at 5 mol% relative to the number of thiol end groups, and the solution was irradiated with 525 nm green light for 6–27.5 minutes depending on the cross-linker, due to variable cross-linker absorption at this wavelength (SI, **Figure S15**). The gelation could not be performed in water due to limited aqueous solubility of the linkers, so the organic solvent was subsequently removed *in vacuo* and the gel re-swelled with 200 µL of aqueous HEPES buffer (0.1 M, pH 7.44). Gels did not form in the absence of cross-linker or Eosin Y, suggesting that disulfide formation is not responsible for network formation under these conditions.

In a frequency sweep, all gels exhibited similar plateau moduli of ~1600 ± 150 Pa, as expected for an associative hydrogel in which cross-link density is dictated by the synthesis conditions rather than the exchange chemistry (**Figure 9b**). Only gel-**MA** underwent crossover between G' and G'' within the experimental frequency range at 1.6 rad/s, consistent with its faster exchange kinetics. The stress relaxation plot of **gel-ctrl** showed slow but evident stress relaxation (τ value of 1553 s), which may be attributed to other modes of stress relaxation such as the reptation of dangling chain ends (**Figure 9c**).[46,47] These networks were synthesized with a large concentration of dangling ends (free thiol) by design to promote the associative exchange reaction. **Gel-MA**, **gel-AA**, and **gel-MM** relaxed all stress faster than **gel-ctrl**, and fitting data to a single element Maxwell model yielded characteristic relaxation times (τ) of 0.672, 173, and 621 s. Thus, the rates of stress relaxation for the cross-linker scope span four orders of magnitude.

Based on the trends obtained from correlating stress relaxation time with Hirshfeld charge (**Figure 10a**; SI, **Figure S36a**) and LUMO (**Figure 10b**; SI, **Figure S36b**), **gel-CH** was predicted to exhibit a τ value of 49.8 s and 53.7 s, respectively. While **gel-CH** relaxed stress on a timescale intermediate to that of **gel-MA** and **gel-AA** as anticipated, its characteristic relaxation time was 115 s, approximately twice the predicted value (**Figure 9c**).

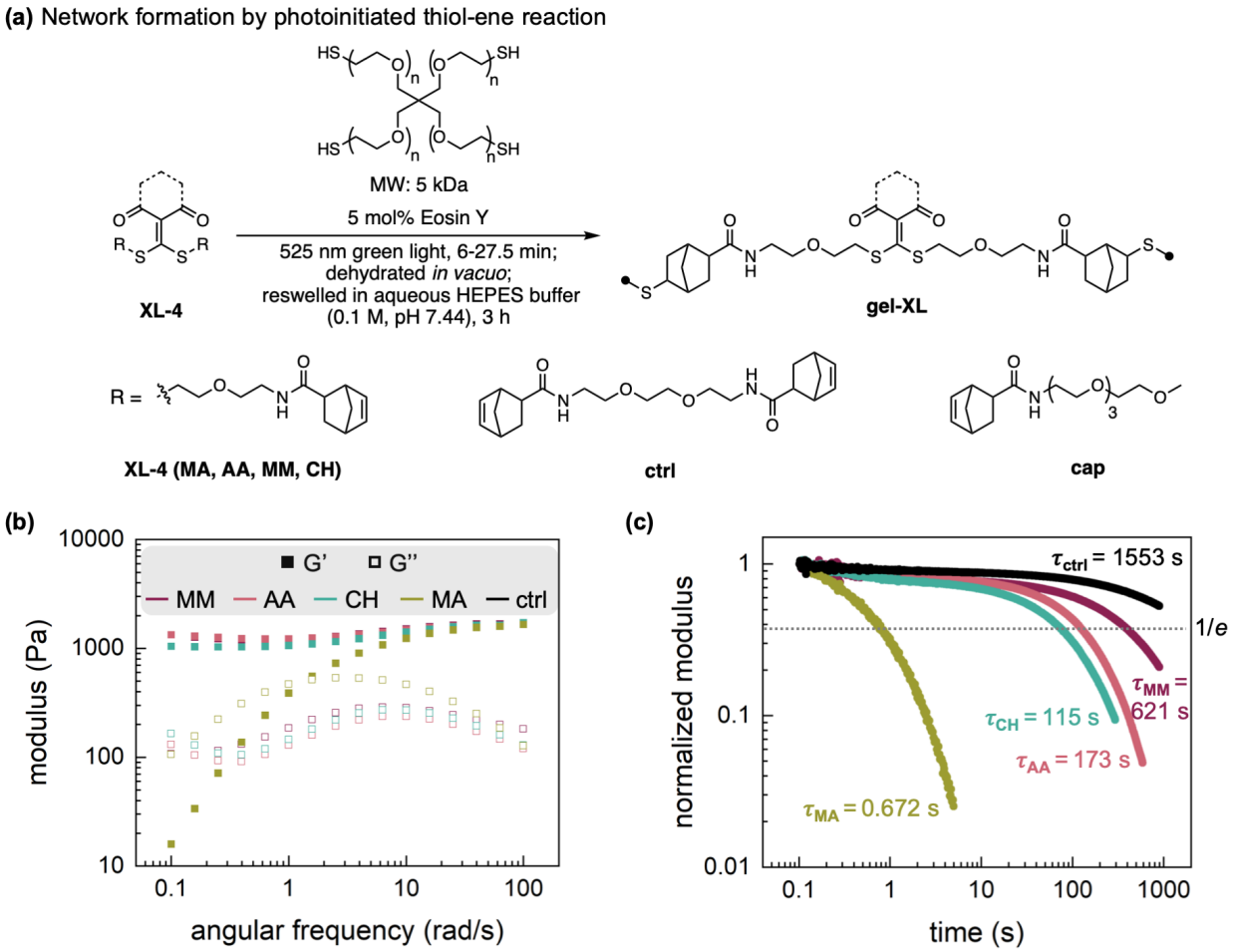

Figure 9. (a) Conditions for network formation by photoinitiated thiol-ene reaction with 4-arm PEG-thiol and structures of the norbornene-terminated cross-linkers. (b) Frequency sweeps of **gel-MA**, **gel-CH**, **gel-AA**, and **gel-MM** in HEPES (10 w/v%, 0.1 M, pH 7.44, 5% strain). (c) Stress relaxation profiles of **gel-MA**, **gel-CH**, **gel-AA**, **gel-MM**, and **gel-ctrl** (5% strain).

Qualitatively, the trend in stress relaxation rate correlates with the rates of small molecule thiol exchange: cross-linkers that exchange faster also relax stress faster. However, while other studies have provided a similar qualitative comparison of small-molecule and mechanical data in associative networks,[48–53] we sought to analyze the scaling relationship quantitatively. In supramolecular networks, time-cross-linker superposition of the frequency sweep data has been applied when there is a 1:1 scaling relationship between G' and G'' with k_d[54] or $E_{a,d}$.[55] This analysis confirms that networks composed of distinct but analogous cross-linkers rearrange through common mechanisms. However, this approach was not compatible with our system because only **gel-MA** displayed a crossover frequency within an experimentally accessible range. Therefore, we instead plotted $1/\tau$ obtained from stress relaxation and small-molecule rate constants (k_{ex}) on a log-log plot, yielding a line with a slope of 1.01 (**Figure S34**). The slope of nearly unity demonstrates that $1/\tau$ is linearly proportional to k_{ex}. These data suggest that stress relaxation in swollen associative networks is predominantly controlled by network exchange and can be quantitatively predicted by trends in cross-link kinetics.[56]

In an associative mechanism, removing the free thiols should inhibit stress relaxation. Therefore, gel-$\mathbf{AA_{cap}}$ was formed with stoichiometric norbornene end-capper **cap**, which reacts with the excess free thiols. Indeed, **gel-AA$_{cap}$** exhibited significantly slower stress relaxation relative to **gel-AA** (τ value of 675 s with **cap**, compared to 173 s without), confirming the associative nature of thiol-dithioalkylidene exchange (**Figure 11c**). The residual stress relaxation suggests that capping may not be quantitative.

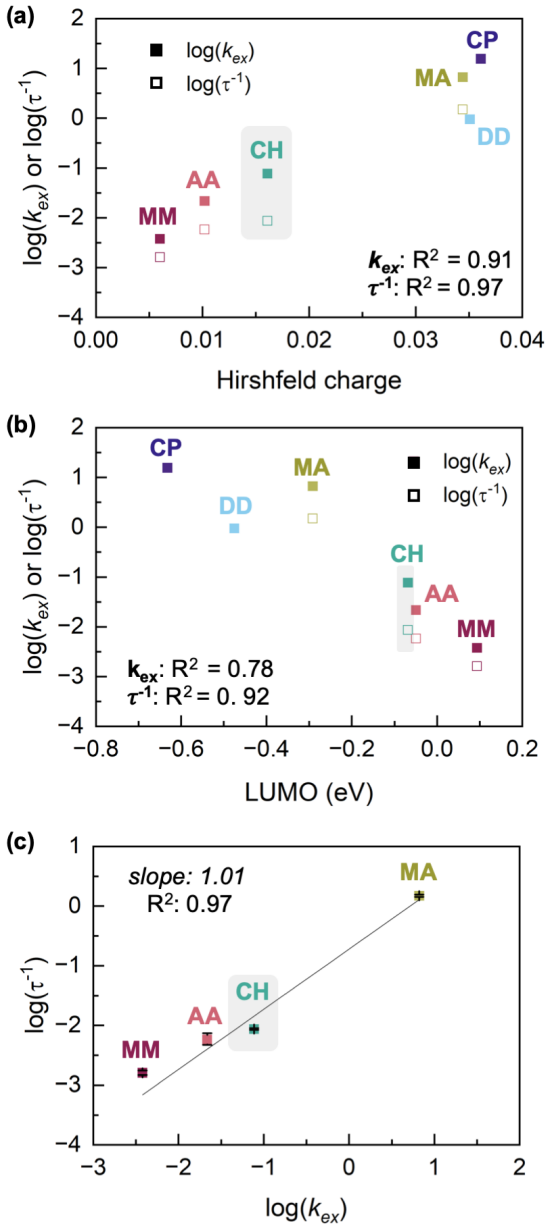

Figure 10. (a,b) Correlation of stress relaxation time scale of **gel-MA**, **gel-CH**, **gel-AA**,and **gel-MM** and k_{ex} of **MA-1**, **AA-1**, **CH-1**, and **MM-1** with (a) Hirshfeld charge and (b) LUMO values. (c) Log-log plot comparing stress relaxation timescale of **gel-MA**, **gel-CH**, **gel-AA**, and **gel-MM** to exchange rate of **MA-1**, **AA-1**, **CH-1**, and **MM-1**. Shaded boxes indicates cross-linker for which reactivity and stress relaxation time were predicted *in silico* before experimental confirmation.

Associative networks such as vitrimers are commonly assumed to resist dissolution in good solvent in the absence of any competitive nucleophiles. However, we[57] and others[51,58,59] have shown that vitrimers can undergo dissolution. As concentration of the polymer network decreases relative to the surrounding medium, successive associative exchange reactions favor intramolecular linkages, disrupting the infinite network structure and dissolving it into soluble hyperbranched loopy polymers (**Figure 11a**). We performed swelling experiments on the hydrogels to evaluate whether such a mechanism for dissolution is possible in this system. When **gel-AA** was suspended in excess buffer, we observed complete dissolution of the gel within 24 hours (**Figure 11b**), while non-dynamic **gel-ctrl** remained stable for at least a week. Subjecting **gel-AA$_{cap}$** to the swelling experiment yielded slower dissolution than **gel-AA** (incomplete dissolution after 5 days), again confirming that free thiols are required to mediate the exchange reactions that lead to hydrogel dissolution, and that hydrolysis is not the major dissolution pathway.

We hypothesize that the dissolved network sample is comprised of multiple species including unimers with primary loops and numerous large, polydisperse polymers. Gel permeation chromatography (GPC) of the dissolved **gel-AA** solution indicated that the dissolution products had increased polydispersity compared to a sample of 4-arm 5 kDa PEG-SH (SI, **Figure S37**). ^{1}H DOSY analysis of 4-arm 5 kDa PEG-SH and dissolved **gel-AA** also suggests that larger species are present in the latter. Diffusion analysis of the PEG monomer methylene proton at 3.66 ppm yielded diffusion constants of 2.54 x 10^{-6} for 4-arm PEG-SH and 1.57 x 10^{-6} for dissolved **gel-AA** (SI, **Table S41**). We anticipate that with longer reaction times, decreased network concentration relative to the surrounding medium, and increased temperature to accelerate equilibration, the networks will dissolve into a more uniform set of products.

Lastly, we demonstrated the capacity of the gels to undergo self-healing, which should also be determined by the rate of associative exchange (k_{ex}). We cut samples of **gel-MA**, **gel-AA**, and **gel-ctrl**, pressed the cut halves together, and qualitatively compared self-healing ability over time (**Figure 12**). **Gel-MA**, which undergoes the fastest cross-link exchange, healed the fastest of the three samples and within minutes could be held against gravity with a spatula. Similarly, **gel-AA** was self-supporting after 30 minutes. While healed, it still displayed a visible seam where the original gel was divided. By comparison, **gel-ctrl** remained unhealed after 2 hours, and an attempt to pick it up resulted in gel refracture. Taken together, these studies demonstrate that both stress relaxation and self-healing rates can be controlled by k_{ex} in associative hydrogels.

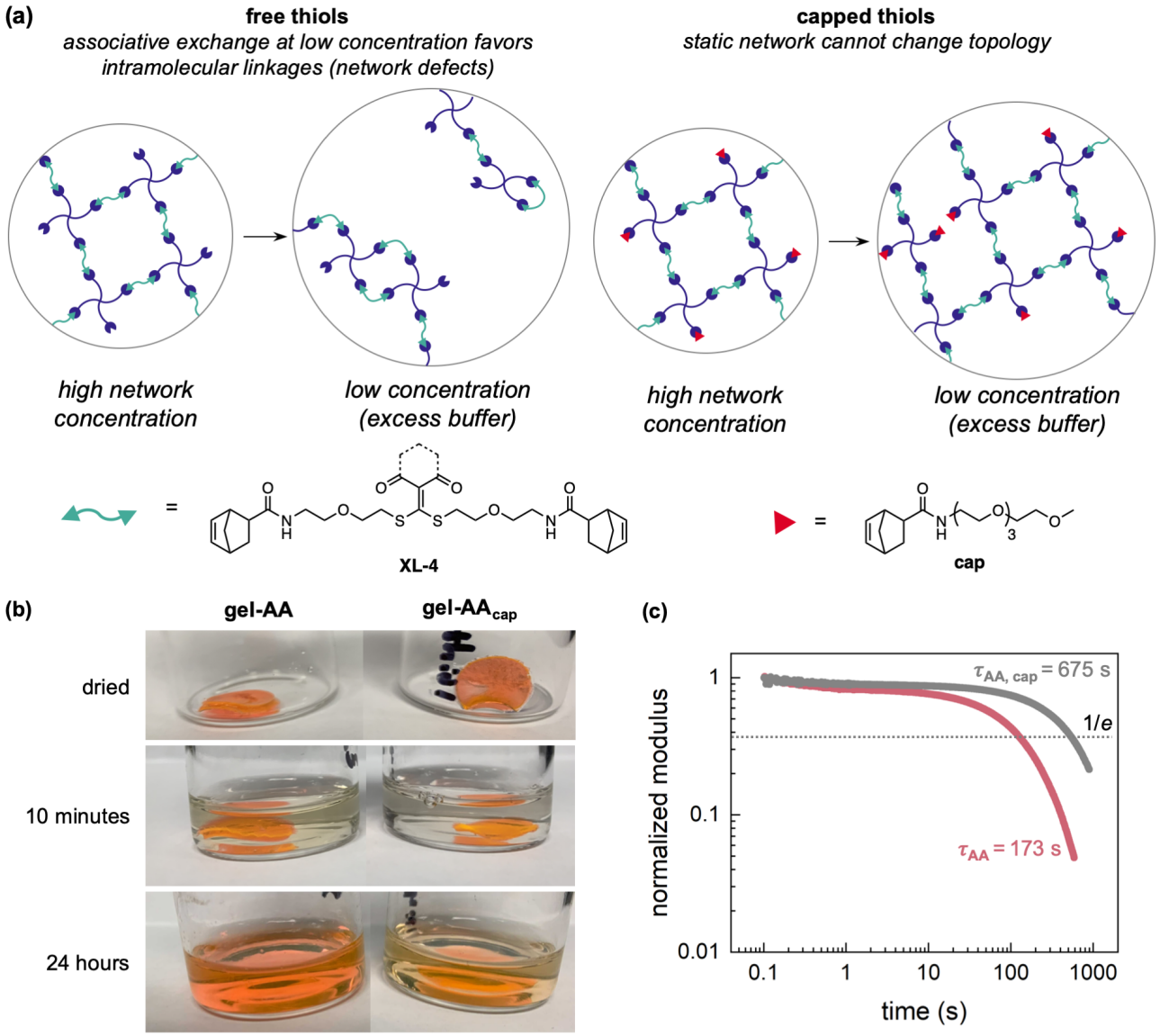

Figure 11. Effects of capping excess thiol on stress relaxation and exchange-mediated network dissolution. (a) Illustration and (b) photographs of exchange-mediated dissolution with or without capping agent cap. (c) Stress relaxation profiles of **gel-AA** and **gel-AA$_{cap}$**.

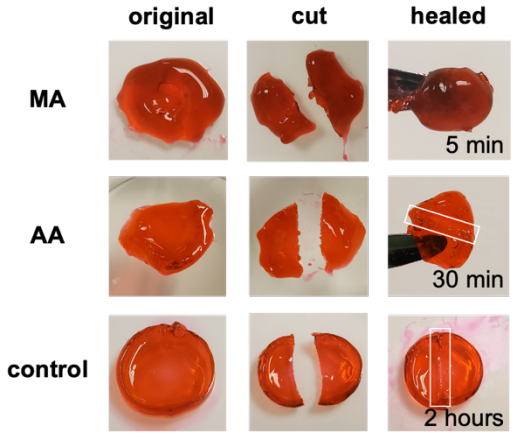

Figure 12. Pictures of **gel-MA**, **gel-AA**, and **gel-ctrl** undergoing self-healing. White boxes outline residual seams.

CONCLUSION

The aqueous reactivity of a family of dithioalkylidenes in associative thiol exchange was investigated and the relationship between structure and reactivity was elucidated. Cyclic compounds were shown to undergo associative exchange faster than their linear analogs due to reduced conformational freedom and greater resonance stabilization of the anionic tetrahedral intermediate. Based on the observed trends with spectroscopic and computational data, the relative reactivity of new dithioalkylidenes may be predicted *in silico* using readily obtained values such as Hirshfeld charge or LUMO values. Cross-linkers with different exchange rates were incorporated into hydrogels and the rates of stress relaxation were quantitatively related to associative exchange rates. We envision that the ease of structural manipulation and predictive reactivity of dithioalkylidenes will motivate their adoption in stress-relaxing hydrogels and other dynamic materials with tunable reconfiguration. Furthermore, we hope that this work emphasizes the utility of quantitative

structure-reactivity-property relationships to predict and understand the properties of dynamic networks.[60,51]

ASSOCIATED CONTENT

Supporting Information

Synthetic procedures, characterization data for new compounds, UV-vis spectra, kinetics data and details of model and fitting, rheological data, computed molecular descriptors (pdf)
XYZ coordinates of calculated structures (xyz)
Summary of calculated energies (xlsx)
Single-crystal X-ray data (cif)

AUTHOR INFORMATION

Corresponding Author

Julia A. Kalow – *Department of Chemistry, Northwestern University, Evanston, Illinois 60208, United States*

Email: jkalow@northwestern.edu

Present Addresses

†If an author's address is different than the one given in the affiliation line, this information may be included here.

ACKNOWLEDGMENT

This work was supported by the NSF Center for the Chemistry of Molecularly Optimized Networks (MONET), CHE-2116298. J.A.K. was supported by a Sloan Research Fellowship and a Dreyfus Teacher-Scholar Award. C.T.E. acknowledges support from a National Science Foundation Graduate Research Fellowship (grant no. DGE-1842165). This work made use of NMR and MS instrumentation at the Integrated Molecular Structure Education and Research Center (IMSERC) at Northwestern, which has received support from the NSF (NSF CHE-9871268), Soft and Hybrid Nanotechnology Experimental (SHyNE) Resource (NSF ECCS-1542205), the State of Illinois, and the International Institute for Nanotechnology. The rheometer used in this work was supported by NSF CHE-1901635, NIH R01GM132677, and Northwestern University. This work used Expanse at San Diego Supercomputing Center through allocation CHE140073 from the Advanced Cyberinfrastructure Coordination Ecosystem: Services and Support (ACCESS) program, which is supported by National Science Foundation Grants #2138259, #2138286, #2138307, #2137603, and #2138296.

REFERENCES

(1) Webber, M. J.; Tibbitt, M. W. Dynamic and Reconfigurable Materials from Reversible Network Interactions. *Nat. Rev. Mater.* **2022**.

(2) Zhang, V.; Kang, B.; Accardo, J. V.; Kalow, J. A. Structure–Reactivity–Property Relationships in Covalent Adaptable Networks. *J. Am. Chem. Soc.* **2022**, *144*, 22358–22377.

(3) Ullah, F.; Othman, M. B. H.; Javed, F.; Ahmad, Z.; Akil, H. Md. Classification, Processing and Application of Hydrogels: A Review. *Mater. Sci. Eng. C* **2015**, *57*, 414–433.

(4) Lee, K. Y.; Mooney, D. J. Hydrogels for Tissue Engineering. *Chem. Rev.* **2001**, *101*, 1869–1880.

(5) Caló, E.; Khutoryanskiy, V. V. Biomedical Applications of Hydrogels. *European Polymer Journal* **2015**, *65*, 252–267.

(6) Wang, H.; Heilshorn, S. C. Adaptable Hydrogel Networks with Reversible Linkages for Tissue Engineering. *Adv. Mater.* **2015**, *27*, 3717–3736.

(7) Rosales, A. M.; Anseth, K. S. The Design of Reversible Hydrogels to Capture Extracellular Matrix Dynamics. *Nat. Rev. Mater.* **2016**, *1*, 15012.

(8) Tang, S.; Richardson, B. M.; Anseth, K. S. Dynamic Covalent Hydrogels as Biomaterials to Mimic the Viscoelasticity of Soft Tissues. *Prog. Mater. Sci.* **2021**, *120*, 100738.

(9) Chaudhuri, O.; Cooper-White, J.; Janmey, P. A.; Mooney, D. J.; Shenoy, V. B. Effects of Extracellular Matrix Viscoelasticity on Cellular Behaviour. *Nature* **2020**, *584*, 535–546.

(10) Tuncaboylu, D. C.; Sari, M.; Oppermann, W.; Okay, O. Tough and Self-Healing Hydrogels Formed via Hydrophobic Interactions. *Macromolecules* **2011**, *44*, 4997–5005.

(11) Jiang, H.; Duan, L.; Ren, X.; Gao, G. Hydrophobic Association Hydrogels with Excellent Mechanical and Self-Healing Properties. *Eur. Polym. J.* No. 112, 660–669.

(12) Harada, A.; Takashima, Y.; Nakahata, M. Supramolecular Polymeric Materials via Cyclodextrin–Guest Interactions. *Acc. Chem. Res.* **2014**, *47*, 2128–2140.

(13) Kakuta, T.; Takashima, Y.; Nakahata, M.; Otsubo, M.; Yamaguchi, H.; Harada, A. Preorganized Hydrogel. *Advanced Materials* **2013**, *25*, 2849–2853.

(14) Appel, E. A.; Biedermann, F.; Rauwald, U.; Jones, S. T.; Zayed, J. M.; Scherman, O. A. Supramolecular Cross-Linked Networks *via* Host–Guest Complexation with Cucurbit[8]Uril. *J. Am. Chem. Soc.* **2010**, *132*, 14251–14260.

(15) Guo, M.; Pitet, L. M.; Wyss, H. M.; Vos, M.; Dankers, P. Y. W.; Meijer, E. W. Tough Stimuli-Responsive Supramolecular Hydrogels with Hydrogen-Bonding Network Junctions. *J. Am. Chem. Soc.* **2014**, *136*, 6969–6977.

(16) Kang, B.; Kalow, J. A. Internal and External Catalysis in Boronic Ester Networks. *ACS Macro Lett.* **2022**, *11*, 394–401.

(17) Accardo, J. V.; McClure, E. R.; Mosquera, M. A.; Kalow, J. A. Using Visible Light to Tune Boronic Acid-Ester Equilibria. *J. Am. Chem. Soc.* **2020**, *142*, 19969–19979.

(18) Accardo, J. V.; Kalow, J. A. Reversibly Tuning Hydrogel Stiffness through Photocontrolled Dynamic Covalent Crosslinks. *Chem. Sci.* **2018**, *9*, 5987–5993.

(19) Barsoum, D. N.; Kirinda, V. C.; Kang, B.; Kalow, J. A. Remote-Controlled Exchange Rates by Photoswitchable Internal Catalysis of Dynamic Covalent Bonds. *J. Am. Chem. Soc.* **2022**, *144*, 10168–10173.

(20) Parada, G. A.; Zhao, X. Ideal Reversible Polymer Networks. *Soft Matter* **2018**, *14*, 5186–5196.

(21) Marco-Dufort, B.; Iten, R.; Tibbitt, M. W. Linking Molecular Behavior to Macroscopic Properties in Ideal Dynamic Covalent Networks. *J. Am. Chem. Soc.* **2020**, *142*, 15371–15385.

(22) Cai, P. C.; Su, B.; Zou, L.; Webber, M. J.; Heilshorn, S. C.; Spakowitz, A. J. Rheological Characterization and Theoretical Modeling Establish Molecular Design Rules for Tailored Dynamically Associating Polymers. *ACS Cent. Sci.* **2022**.

(23) FitzSimons, T. M.; Oentoro, F.; Shanbhag, T. V.; Anslyn, E. V.; Rosales, A. M. Preferential Control of Forward Reaction Kinetics in Hydrogels Crosslinked with Reversible Conjugate Additions. *Macromolecules* **2020**, *53*, 3738–3746.

(24) Winne, J. M.; Leibler, L.; Du Prez, F. E. Dynamic Covalent Chemistry in Polymer Networks. *Polym. Chem.* **2019**, *10*, 6091–6108.

(25) Diehl, K. L.; Kolesnichenko, I. V.; Robotham, S. A.; Bachman, J. L.; Zhong, Y.; Brodbelt, J. S.; Anslyn, E. V. Click and Chemically Triggered Declick Reactions through Reversible Amine and Thiol Coupling via a Conjugate Acceptor. *Nat. Chem.* **2016**, *8*, 968–973.

(26) Ishibashi, J. S. A.; Kalow, J. A. Vitrimeric Silicone Elastomers Enabled by Dynamic Meldrum's Acid-Derived Cross-Links. *ACS Macro Lett.* **2018**, *7*, 482–486.

(27) El-Zaatari, B. M.; Ishibashi, J. S. A.; Kalow, J. A. Cross-Linker Control of Vitrimer Flow. *Polym. Chem.* **2020**, *11*, 5339–5345.

(28) Sun, X.; Chwatko, M.; Lee, D.-H.; Bachman, J. L.; Reuther, J. F.; Lynd, N. A.; Anslyn, E. V. Chemically Triggered Synthesis, Remodeling, and Degradation of Soft Materials. *J. Am. Chem. Soc.* **2020**, *142*, 3913–3922.

(29) Feng, X.; Wu, T.; Sun, X.; Qian, X. "Indanonalkene" Photoluminescence Platform. *J. Am. Chem. Soc.* **2021**, *143*, 21622–21629.

(30) Chang, L.; Wang, C.; Han, S.; Sun, X.; Xu, F. Chemically Triggered Hydrogel Transformations through Covalent Adaptable Networks and Applications in Cell Culture. *ACS Macro Lett.* **2021**, *10*, 901–906.

(31) Brown, T. E.; Carberry, B. J.; Worrell, B. T.; Dudaryeva, O. Y.; McBride, M. K.; Bowman, C. N.; Anseth, K. S. Photopolymerized Dynamic

Hydrogels with Tunable Viscoelastic Properties through Thioester Exchange. *Biomaterials* **2018**, *178*, 496–503.

(32) Carberry, B. J.; Rao, V. V.; Anseth, K. S. Phototunable Viscoelasticity in Hydrogels Through Thioester Exchange. *Ann. Biomed. Eng.* **2020**, *48*, 2053–2063.

(33) Worrell, B. T.; Mavila, S.; Wang, C.; Kontour, T. M.; Lim, C.-H.; McBride, M. K.; Musgrave, C. B.; Shoemaker, R.; Bowman, C. N. A User's Guide to the Thiol-Thioester Exchange in Organic Media. *Polym. Chem.* **2018**, *9*, 4523–4534.

(34) Bracher, P. J.; Snyder, P. W.; Bohall, B. R.; Whitesides, G. M. The Relative Rates of Thiol–Thioester Exchange and Hydrolysis for Alkyl and Aryl Thioalkanoates in Water. *Orig. Life Evol. Biosph.* **2011**, *41*, 399–412.

(35) Davis, G. J.; Sofka, H. A.; Jewett, J. C. Highly Stable Meldrum's Acid Derivatives for Irreversible Aqueous Covalent Modification of Amines. *Org. Lett.* **2020**, *22*, 2626–2629.

(36) Arnett, E. M.; Harrelson, J. A. Ion Pairing and Reactivity of Enolate Anions. 7. A Spectacular Example of the Importance of Rotational Barriers. *J. Am. Chem. Soc.* **1987**, *109*, 809–812.

(37) Arnett, E. M.; Maroldo, S. G.; Schilling, S. L.; Harrelson, J. A. Ion Pairing and Reactivity of Enolate Anions. 5. Thermodynamics of Ionization of .Beta.-Di- and Tricarbonyl Compounds in Dimethyl Sulfoxide Solution and Ion Pairing of Their Alkali Salts. *J. Am. Chem. Soc.* **1984**, *106*, 6759–6767.

(38) Wiberg, K. B.; Laidig, K. E. Acidity of (Z)- and (E)-Methyl Acetates. *J. Am. Chem. Soc.* **1988**, *110*, 1872–1874.

(39) Wang, Xuebao.; Houk, K. N. Theoretical Elucidation of the Origin of the Anomalously High Acidity of Meldrum's Acid. *J. Am. Chem. Soc.* **1988**, *110*, 1870–1872.

(40) Byun, K.; Mo, Y.; Gao, J. New Insight on the Origin of the Unusual Acidity of Meldrum's Acid from Ab Initio and Combined QM/MM Simulation Study. *J. Am. Chem. Soc.* **2001**, *123*, 3974–3979.

(41) Knizia, G. Intrinsic Atomic Orbitals: An Unbiased Bridge between Quantum Theory and Chemical Concepts. *J. Chem. Theory Comput.* **2013**, *9*, 4834–4843.

(42) Knizia, G.; Klein, J. E. M. N. Electron Flow in Reaction Mechanisms—Revealed from First Principles. *Angewandte Chemie International Edition* **2015**, *54*, 5518–5522.

(43) Liu, S. Quantifying Reactivity for Electrophilic Aromatic Substitution Reactions with Hirshfeld Charge. *J. Phys. Chem. A* **2015**, *119*, 3107–3111.

(44) Liu, S.; Rong, C.; Lu, T. Information Conservation Principle Determines Electrophilicity, Nucleophilicity, and Regioselectivity. *J. Phys. Chem. A* **2014**, *118*, 3698–3704.

(45) Wang, B.; Rong, C.; Chattaraj, P. K.; Liu, S. A Comparative Study to Predict Regioselectivity, Electrophilicity and Nucleophilicity with Fukui Function and Hirshfeld Charge. *Theor. Chem. Acc.* **2019**, *138*, 124.

(46) Curro, J. G.; Pincus, P. A Theoretical Basis for Viscoelastic Relaxation of Elastomers in the Long-Time Limit. *Macromolecules* **1983**, *16*, 559–562.

(47) Curro, J. G.; Pearson, D. S.; Helfand, E. Viscoelasticity of Randomly Crosslinked Polymer Networks. Relaxation of Dangling Chains. *Macromolecules* **1985**, *18*, 1157–1162.

(48) Cromwell, O. R.; Chung, J.; Guan, Z. Malleable and Self-Healing Covalent Polymer Networks through Tunable Dynamic Boronic Ester Bonds. *J. Am. Chem. Soc.* **2015**, *137*, 6492–6495.

(49) Nishimura, Y.; Chung, J.; Muradyan, H.; Guan, Z. Silyl Ether as a Robust and Thermally Stable Dynamic Covalent Motif for Malleable Polymer Design. *J. Am. Chem. Soc.* **2017**, *139*, 14881–14884.

(50) Denissen, W.; Droesbeke, M.; Nicolaÿ, R.; Leibler, L.; Winne, J. M.; Du Prez, F. E. Chemical Control of the Viscoelastic Properties of Vinylogous Urethane Vitrimers. *Nat. Commun.* **2017**, *8*, 14857.

(51) Schoustra, S. K.; Dijksman, J. A.; Zuilhof, H.; Smulders, M. M. J. Molecular Control over Vitrimer-like Mechanics – Tuneable Dynamic Motifs Based on the Hammett Equation in Polyimine Materials. *Chem. Sci.* **2021**, *12*, 293–302.

(52) Porath, L.; Huang, J.; Ramlawi, N.; Derkaloustian, M.; Ewoldt, R. H.; Evans, C. M. Relaxation of Vitrimers with Kinetically Distinct Mixed Dynamic Bonds. *Macromolecules* **2022**, *55*, 4450–4458.

(53) Porath, L.; Soman, B.; Jing, B. B.; Evans, C. M. Vitrimers. *ACS Macro Lett.* **2022**, *11*, 475–483.

(54) Yount, W. C.; Loveless, D. M.; Craig, S. L. Small-Molecule Dynamics and Mechanisms Underlying the Macroscopic Mechanical Properties of Coordinatively Cross-Linked Polymer Networks. *J. Am. Chem. Soc.* **2005**, *127*, 14488–14496.

(55) Appel, E. A.; Forster, R. A.; Koutsioubas, A.; Toprakcioglu, C.; Scherman, O. A. Activation Energies Control the Macroscopic Properties of Physically Cross-Linked Materials. *Angew. Chem. Int. Ed.* **2014**, *53*, 10038–10043.

(56) Ricarte, R. G.; Shanbhag, S. Unentangled Vitrimer Melts. *Macromolecules* **2021**, *54*, 3304–3320.

(57) Ishibashi, J. S. A.; Pierce, I. C.; Chang, A. B.; Zografos, A.; El-Zaatari, B. M.; Fang, Y.; Weigand, S. J.; Bates, F. S.; Kalow, J. A. Mechanical and Structural Consequences of Associative Dynamic Cross-Linking in Acrylic Diblock Copolymers. *Macromolecules* **2021**, *54*, 3972–3986.

(58) Breuillac, A.; Kassalias, A.; Nicolaÿ, R. Polybutadiene Vitrimers Based on Dioxaborolane Chemistry and Dual Networks with Static and Dynamic Cross-Links. *Macromolecules* **2019**, *52*, 7102–7113.

(59) Hajj, R.; Duval, A.; Dhers, S.; Avérous, L. Network Design to Control Polyimine Vitrimer Properties. *Macromolecules* **2020**, *53*, 3796–3805.

(60) Van Herck, N.; Maes, D.; Unal, K.; Guerre, M.; Winne, J. M.; Du Prez, F. E. Covalent Adaptable Networks with Tunable Exchange Rates Based on Reversible Thiol–Yne Cross-Linking. *Angewandte Chemie* **2020**, *132*, 3637–3646.

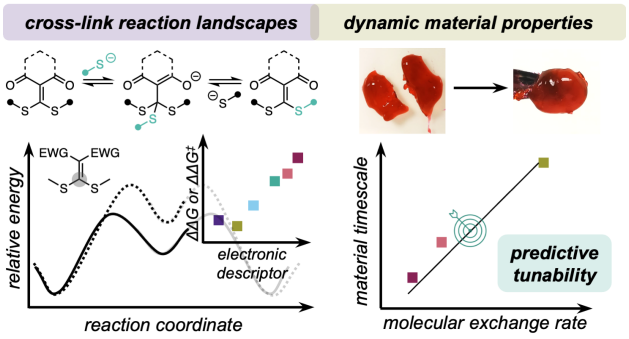
cross-link reaction landscapes
dynamic material properties
EWG
EWG
relative energy
ΔΔG or ΔΔG‡
electronic descriptor
reaction coordinate
material timescale
molecular exchange rate
predictive tunability